Testing a Prototype Ion Probe for Europa's Plasma Interaction: Colorado Europa Langmuir Probe

Shawn Beckman

A senior honors thesis submitted in partial

fulfillment for the Honors Physics

Bachelors of Arts Degree at the

University of Colorado

College of Arts and Sciences

November 2014

Committee Members:

Thesis Advisor: Professor Robert Ergun, Department of Astrophysical and Planetary Sciences

Professor John Cumalat, Department of Physics

Professor James Nagle, Department of Physics

Abstract

The Colorado Europa Langmuir Probe (CELP) is a plasma instrument designed to characterize Europa's plasma interaction to derive external magnetic fields. In order to accomplish the proposed science goal, CELP must be able to measure ion density, temperature, and flow direction. To do this, a design similar to a cylindrical Faraday Cup is utilized, using three selection grids and four collecting surfaces. Necessary capabilities of the instrument include angular reconstruction in the yaw axis (theta) with respect to an ion beam, and in the roll axis (phi), both with picoamp current resolution. This study involved testing a prototype Ion Langmuir Probe using an ion beam in the lab. Data analysis shows angular resolutions of $\pm 10^{\circ}$ in theta and $\pm 5^{\circ}$ in phi [1] at ion temperatures of 400 eV and 900 eV, with currents on the order of 0.01 nA and 100 nA. The instrument must also show current resolution as low as the minimum expected ionospheric currents at Europa of 10 pA/cm^2 [2]. Using our experimental setup, current resolution at values as low as 0.1 pA/cm^2 was observed. Along with achieving angular and current resolution goals, plots were produced that successfully match experimental data with analytical and simulation models, and the specified goals were achieved.

Contents

Figures

Acknowledgments

First and foremost I would like to thank Prof. James Nagle. Jamie not only provided me with my first job in a research lab, he led by example, teaching me not only to be critical and discerning in my work, but also to unerringly interpret the scientific significance of my experimental results. Jamie's guidance and patience enabled my successful undergraduate research career, for which I cannot thank him enough.

Secondly I would like to thank my thesis advisor and Co-I of CELP, Prof. Robert Ergun. He introduced me to space plasmas in his Solar and Space Physics course two years before I joined the CELP team, and he gave me my first job at LASP shortly after taking his course. The experience I have gained as a direct result has proven invaluable.

The P.I. of CELP, Prof. Fran Bagenal has also been a significant influence on the direction my research experience has taken. Having taken two courses from Fran, I can safely say she is my favorite professor at the university. My final project in one of her classes looked at Europa's sputtered atmosphere, and as a result, I was the first person she emailed about the CELP job opportunity. This was the most exciting email I had ever received, and the project has been the most captivating that I have had the privilege of working on. I owe her many thanks for this one of a kind opportunity.

Last but not least I would like to thank the group of undergrads that have shared a range of emotions with me through our diverse experiences. We have been through Dark Times and happy times, and I can only hope to work professionally with all of them at some point in my career. In particular I would like to thank my CELP colleague and fellow undergrad Jesse Caldwell. Working in the lab with Jesse not only provided a more productive work environment, but a more entertaining one. Without Jesse's help what we accomplished would not have been possible.

Chapter 1

Introduction

The Colorado Europa Langmuir Probe (CELP) is a plasma instrument proposed for NASA's Europa Clipper mission. The Europa Clipper mission is slated to be a flagship mission with the goal of exploring and investigating Europa's habitability [3]. Objectives include characterizing Europa's ice shell and subsurface ocean, understanding the habitability of the subsurface ocean by learning about its composition and chemistry, and understanding the factors that contribute to the development of particular surface features.

Europa's ocean signature was detected by the Galileo spacecraft and can be seen in its magnetometer data [4]. In order to further understand these ocean currents however, precise distinction between ocean signatures and signatures due to Europa's plasma interaction with Jupiter's magnetosphere is required. In short, the CELP instrument will extract the plasma parameters necessary to compute the external currents of Europa's plasma interaction with the Jovian torus. With these data one can determine the externally induced magnetic field.

The external field can be removed using magnetometer data to isolate fields caused by induction in the subsurface ocean.

In this section, Europa's plasma interaction will be discussed in further detail, along with how CELP improves on the design of a more typical plasma instrument, the Langmuir Probe. Enumeration of project CELP's experimental goals along with prototype data goals follow.

1.1 Europa's Plasma Interaction

When looking at precise perturbations in the magnetic fields around Europa to determine induction currents, one must take into account Europa's plasma interaction with the Jovian magnetosphere. This can contribute up to 200 nT in Jupiter's current sheet as compared to the field from induction currents, which are around 250 nT [5]. Characterizing this interaction is crucial in defining induction currents arising from the internal conductivity of Europa. These currents occur when a background, or primary magnetic field that varies in time creates eddy currents inside of the moon near its surface [5]. The eddy currents create a field, which opposes the primary field inside of the moon, causing the field to deflect around the moon.

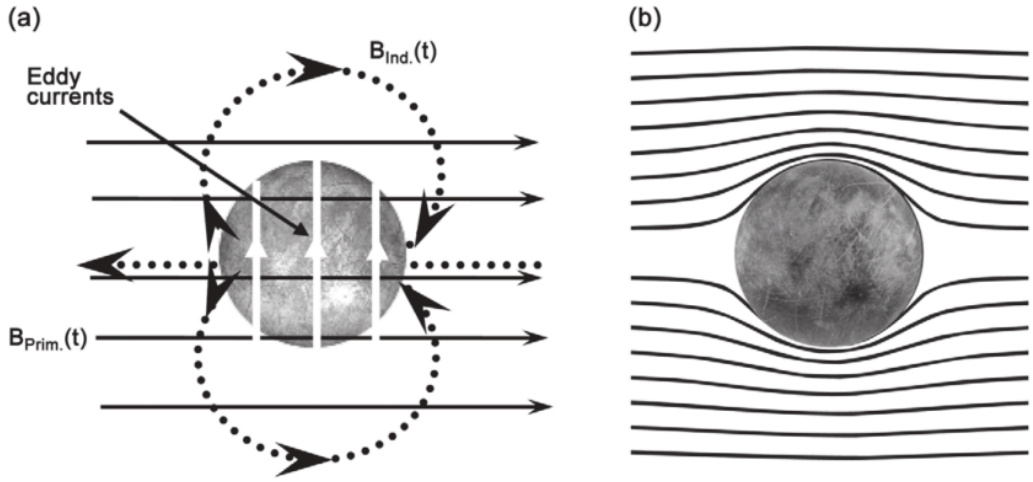

Figure 1.1 [5]: Europa's induction currents:
A primary magnetic field (solid black arrows) produces eddy currents (white arrows), which generate an induced field (black dotted arrows).

Europa's plasma interaction is primarily affected by Europa's atmosphere interacting with plasma in Jupiter's magnetosphere from the Io plasma torus [6]. The incoming plasma is deflected by Europa's ionosphere to produce Alvén wings [7], as seen in Figure 1.2. The ionosphere of Europa is created by electron impact ionization of neutrals in Europa's atmosphere and charge exchange [2]. Charge exchange occurs when a charged particle transfers its charge to a neutral. Separation of currents caused by this interaction and the internal induction must be performed in order to precisely determine induction currents from Europa's ocean. Precise determination of induction currents allows more accurate knowledge of the conductivity of Europa's interior. Knowing more about the conductivity along with data provided by other instruments on the satellite will provide insight into the thickness of the ice crust and the composition of the oceans within.

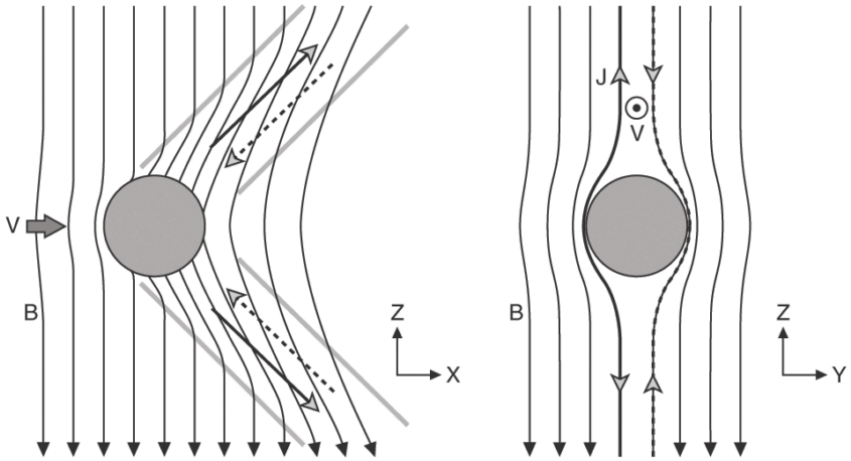

Figure 1.2 [7]: Alfvén wings

1.2 CELP ILP Design

CELP consists of a spherical Langmuir probe and a cylindrical Ion Langmuir Probe (ILP) as shown in Figure 1.3. The tests performed in this experiment are focused on CELP's ILP.

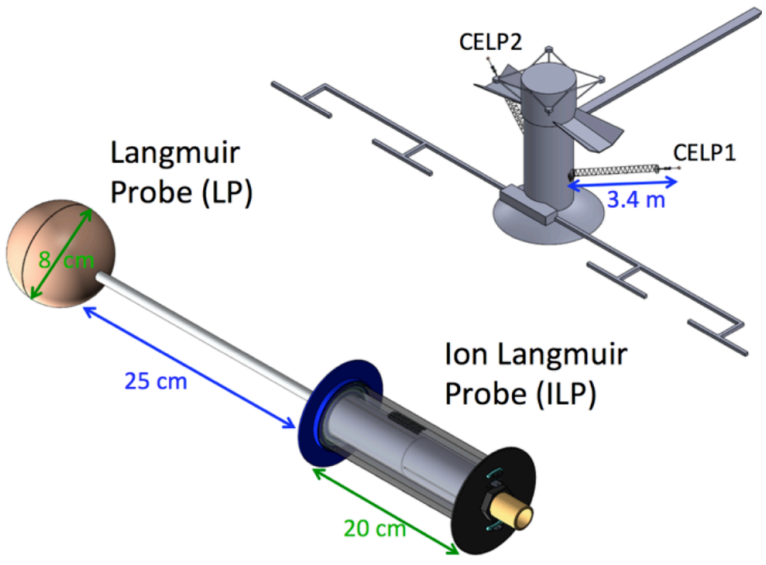

Figure 1.3: CELP Instrument drawing with spacecraft depiction (dimensions for proposed instrument, not for tested prototype)

The ILP is functions like a cylindrical Faraday cup with four collecting surfaces, each with their own independent signal. Unlike the instrument that is shown in Figure 1.3, the prototype instrument has collecting surfaces that are aligned with each other, rather than rotated by 90°. Comparing the collecting surfaces of the ILP in Figure 1.3 to those in Figure 1.4 depicts this. Outside of the collectors lie three concentric, transparent mesh grids. The grids are made out of 85% transparent hexagonal mesh and act as filters for the plasma when a bias voltage is applied. High voltage is supplied to the ILP's inner and middle grids while the outer grid is held at a lower bias. Holding the inner and outer grids at fixed negative potentials, the middle grid, or selection grid, is swept from low to high positive voltages while the collecting surfaces are held at ground. This results in a filtering of the plasma and allows for characterization of different species or energies within the plasma when plotted on an I-V curve. This configuration also allows for rejection of electrons that would normally overwhelm the ion current. A typical I-V curve will consist of the total current that a collector sees plotted against the sweeping voltage applied to the middle grid.

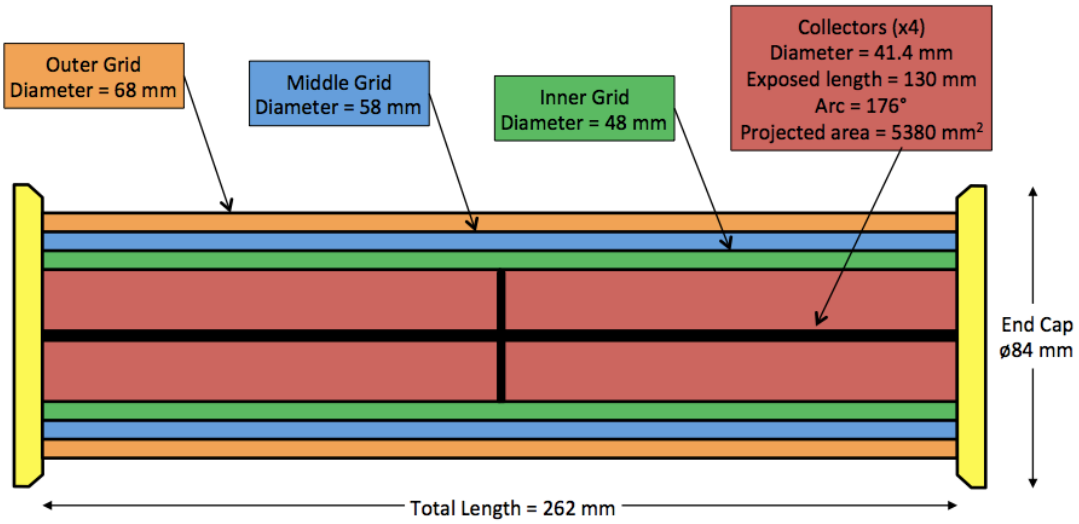

Figure 1.4: ILP Diagram with dimensions

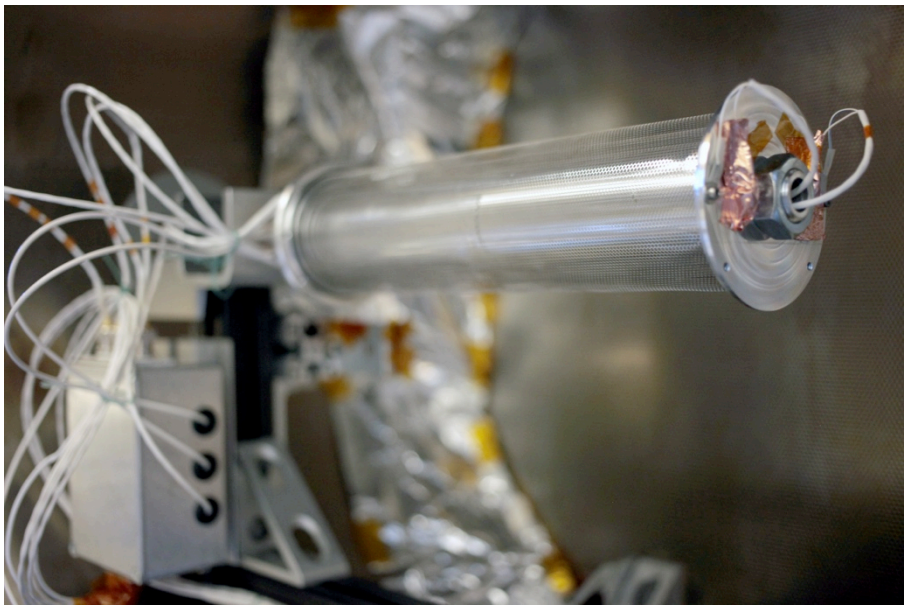

Figure 1.5: Image of CELP ILP prototype
White cables go to the preamp box mounted on the side of the rotational stage.

The CELP preamp, built by Elizabeth Devito (LASP), was designed to measure current ranges of 10^{-12} amps to 10^{-8} amps before saturating the op-

amps. Current from the collectors travels through a feedback resistor (R8 in Figure 1.6), and the voltage across the feedback resistor is amplified and read out.

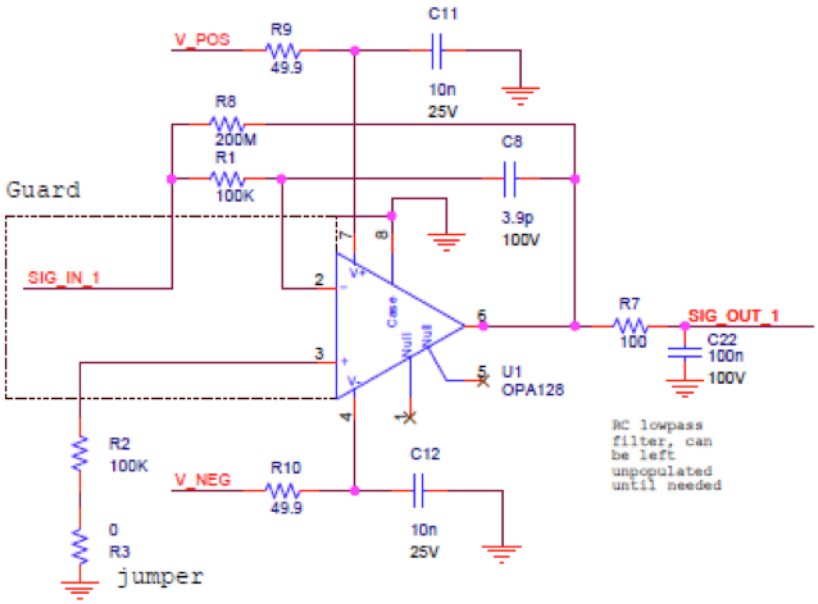

Figure 1.6 – CELP preamp schematic

1.3 Experimental Goals

One of the science goals of the CELP ILP is to measure ion densities (n_i), along with ion temperatures (T_i). Precise values of energy (E) and current density (J) can be extracted from I-V plots assuming adequate current resolution.

$$n = \frac{J}{v} \tag{1.1}$$

$$T = \frac{m{v_{thermal}}^2}{k} \tag{1.2}$$

$$v = \sqrt{\frac{2E}{m}} \tag{1.3}$$

Ion current levels are expected to range from a minimum of 0.01 nA/cm^2 to a maximum of 1.0 nA/cm^2 in Europa's ionosphere and in Jupiter's nearby plasma torus [2]. In this current range, CELP will measure the magnitude of the ion flow velocity (v), and will extract directionality as well. With two ILPs on the spacecraft oriented 124° from each other, CELP will be able to distinguish plasma flow in all directions with a 3.7π str field of view. A standard Langmuir probe cannot measure ion velocity, as electrons obscure the ion signal. Plugging (1.3) into (1.1) shows that a smaller mass results in a larger current density, explaining electron dominance. The ILP will filter out these electrons, as well as electrons from impact ionization and photoionization, which appear as noise, and measure the pure ion signal.

The range of current necessary to satisfy experimental goals is 0.01 nA/cm^2 to 1.0 nA/cm^2. Testing sought achieve these current goals and to create plots from which current resolutions can be derived at two different ion temperatures and two different current levels, while matching analytical and simulated models.

Chapter 2

Experimental Setup

Testing the functionality of the prototype sensor required several elements. The vast majority of the prototype project consisted in building and fine-tuning our setup and test environment, the specifics of which will be discussed in this chapter.

To start, it was necessary to simulate a plasma environment. This entailed creating vacuum and using an ion beam. Once a vacuum chamber big enough to fit the probe was found and an ion source was obtained, rotational stages were installed to simulate various plasma flow directions. Once this was achieved, voltage sources were acquired for the various grid biases, and a data acquisition was set up to control both voltage sweeps on the probe's middle grid and to record our data.

To show that our setup was generally behaving the way we expected it to, we used an instrument called an Ion Energy Analyzer (IEA) in conjunction with the CELP instrument. Using the IEA substantiated the results found with the

CELP instrument and allowed us to look at the plasma environment before testing with the ILP began.

Initial tests revealed problems with our plasma environment that needed to be addressed before data taking began. Problems included high pressure in the chamber while operating at the low current limit on the ion source, which resulted in a higher than the desired current for the ILP, along with undesired features in the data. These problems and their requisite solutions are examined in this chapter.

2.1 Simulating Magnetospheric Plasma Flow

Testing the ILP required a plasma environment that was similar to conditions that the Europa Clipper spacecraft will experience at Europa. This meant testing in vacuum and creating a plasma beam. A 0.83 m^3 vacuum chamber was utilized along with a Kaufman & Robinson (KRI) KDC 100 ion source.

2.1.1 Vacuum Chamber

The vacuum chamber used for the experiment (shown in Figure 2.1) is a 0.83 m^3 cylindrical chamber, measuring 183 cm in length and 76 cm in diameter. The chamber provided sufficient space to fit all of the necessary components of the experiment. The chamber also provided a variety of flange sizes and locations, aiding in the construction of the experiment inside the chamber.

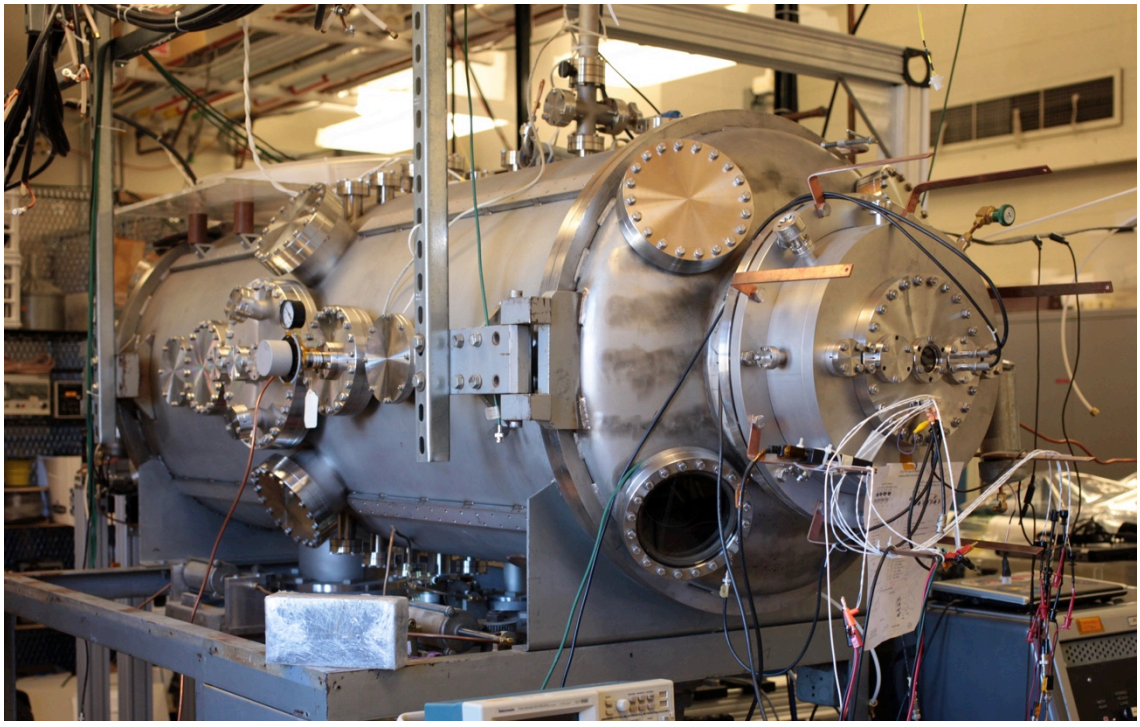

Figure 2.1: Vacuum chamber used for prototype testing

Such a large volume vacuum chamber requires significant pumping power. Attached to the tank are two Varian VHS-10 diffusion pumps (shown in Figure 2.2) which are sufficient to reach a vacuum of 10^{-7} Torr. Diffusion pumps spray hot oil with a downward trajectory into the body of the pump, which imparts a downward momentum on any molecules inside of the pump. The molecules are then compressed by the cooled walls of the vessel and expelled through the fore-line. The pumps are water cooled by a Lytron RC405 water chiller.

Figure 2.2: Diffusion pumps

For reasons detailed later in this chapter, a TMH 520 turbo was installed at one end of the chamber (pictured in Figure 2.3) in the later stages of the experiment. Turbo pumps work by imparting momentum directed away from the vacuum chamber on particles that come into contact with its spinning blades. Given the proper conditions and chamber size, this turbo is capable of reaching 3.8×10^{-11} Torr [8]. With the turbo attached, the base pressure was lowered by 50%. Safety precautions were implemented such that in the event of a power surge, the turbo rough-line (connected to a roughing pump at higher pressure than the chamber) would stay closed, and the turbo would switch back on immediately after the surge.

Figure 2.3: Turbo pump

To achieve vacuum, a roughing pump first pumps the chamber down to a pressure low enough either to turn the turbo on without causing damage to it, or to close the vessel and maintain a sufficiently low pressure while the diffusion pumps are warming up if the turbo is not being used. The necessary temperatures are achieved in the diffusion pumps by cooling the sides of the pumps with a refrigeration unit (aiding the water chiller), and heating the oil with an internal heater to a temperature of 190°C. Once the appropriate temperatures are reached, the main gates of the chamber can be opened so that the diffusion pumps can further pump down the chamber.

2.1.2 Ion Source

The other integral piece in simulating our plasma environment is the ion source, which was provided by Kaufman and Robinson. The ion source was coupled with a KSC 1212 power supply controller.

In short, gas is ionized inside of the source and accelerated into the chamber to create a divergent beam [9]. The ion source however was designed for currents higher than needed to test the ILP, so measures were taken to decrease the current, as discussed later in Section 2.3.2. Both helium and argon were used to create plasmas in this experiment.

Once gas is flowing, discharge can be enabled with the appropriate discharge settings. This means that current is run through a cathode and the gas inside the source is ionized. Once discharge is achieved and beam settings are entered, the beam can be activated. This biases a series of acceleration grids and runs current through a neutralizer, which ensures a neutral plasma by emitting hot electrons from a tungsten wire [10].

Flow rate of the gases into the chamber directly affects the pressure inside of the chamber. Higher pressure in the camber can lead to negative effects such as charge exchange and ionized neutrals, both of which will be explained in detail later in Section 2.3.3. In conjunction with a KSC auto controller flow control unit, a Brooks 5850E mass flow controller (MFC) was utilized to achieve flow rates as low as 0.9 sccm with Ar without losing discharge in the ion source.

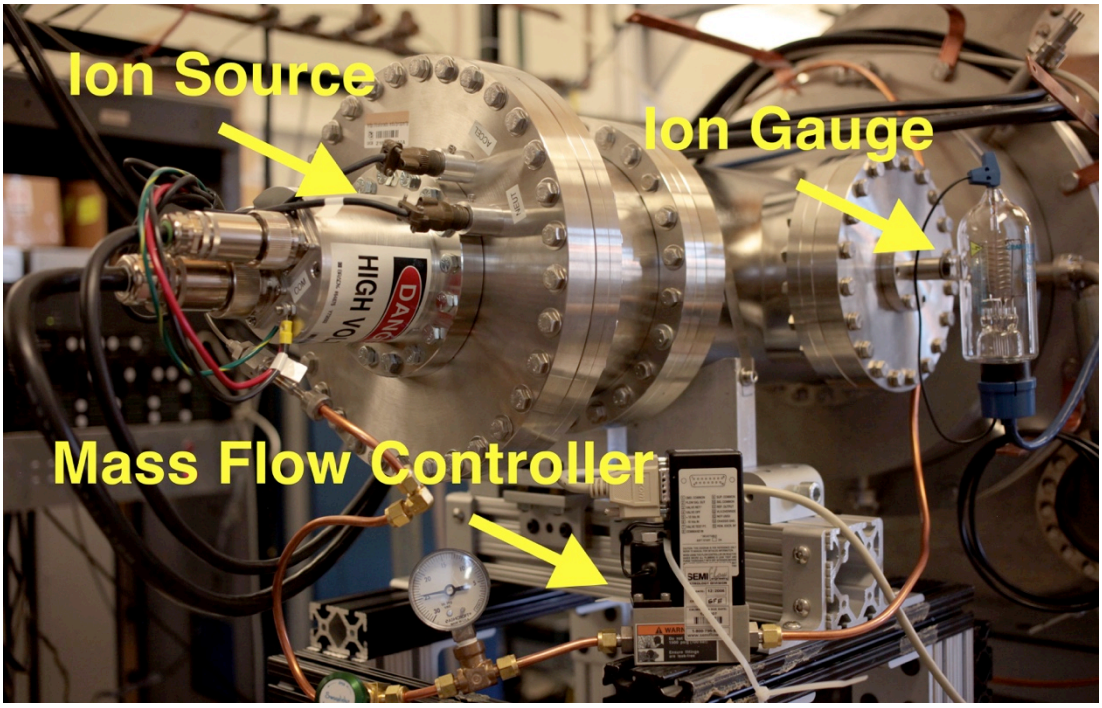

Figure 2.4: Ion source, mass flow controller and ion gauge

Figure 2.5: Ion gauge controller, flow controller, ion source controller (from top to bottom)

2.2 Mechanical Setup & Electronics

To test plasma flow directionality precision, the ability to rotate the probe in theta and phi under vacuum was required. Along with rotational stages, particular electronic instruments and interfaces were required to not only provide voltage where necessary, but to control voltages sweeps, data taking, as well as perform other crucial functions. Diagrams showing the rotations can be seen in Figures 2.7 and 2.8.

2.2.1 Rotational Stages

Two different rotational stages were assembled to accomplish rotations in both theta and phi. Both utilized a MDC CRPP-1 rotational feedthrough, and 1/4" flexible driveshafts to transfer rotation from the chamber wall to the ILP. Because the driveshafts required a moderate amount of torque, a rotational feedthrough utilizing bellows could not be used. Rather, the feedthrough features a direct connection design where a 1/4" rod goes through the feedthrough directly into the chamber. A double O-ring seal coupled with a roughing pump attached to the feedthrough (shown in Figure 2.6) provided sufficient leak prevention under rotation. On the inside of the chamber, the 1/4" rod is connected to a flexible driveshaft used to rotate the instrument. The rig in which the rotational stages are connected was designed such that when the ILP is horizontally mounted, its center lies in the exact center of the chamber. It was also designed so that all rotations were symmetric, i.e. the axis of rotation in theta is aligned

with the center of the probe so that oppositely oriented collecting surfaces occupy the same space after rotation.

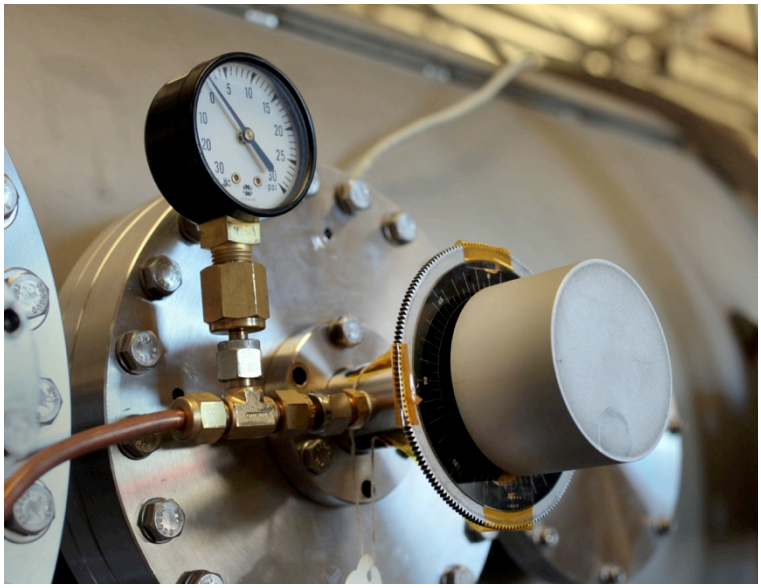

Figure 2.6: Rotational feedthrough

Theta rotations employed a geared rotating plate attached with a 1/4" attachment to connect the flexible driveshaft to (shown in Figure 2.9). This allowed for an angular resolution in theta of 4°, limited by the size of the gear in the rotational plate to which the apparatus was mounted and the play in the flexible driveshaft. Smooth rotation of the theta stage required vacuum-safe lubricant for the geared plate, and particular routing of the flexible drive shaft so that it did not bend and kink under high torque.

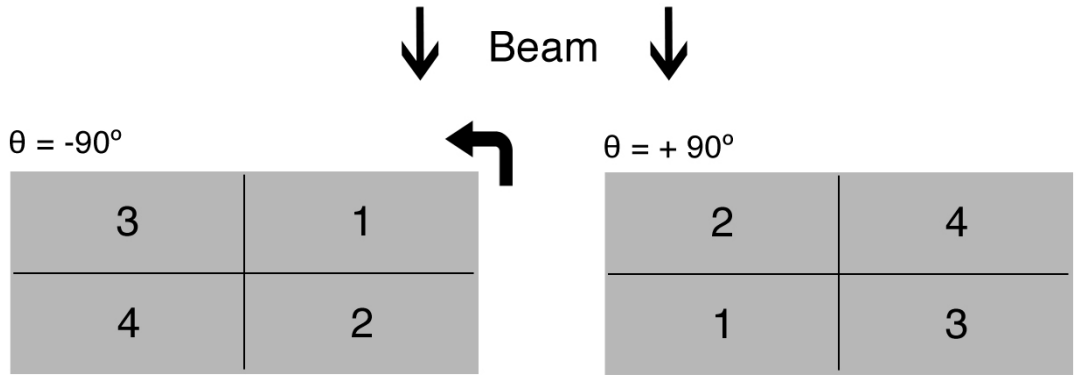

Figure 2.7: Diagram of theta rotation (collectors labeled 1-4)

For rotations in phi, the flexible driveshaft was connected to a small gear, which was then connected to a larger gear attached to the phi rotational axis of the ILP (shown in Figure 2.9). This gearing allowed for an angular resolution in phi of 5°, limited by the size of the gears used and the play in the flexible driveshaft. Some routing of the flexible driveshaft was required to ensure that it did not obscure the collecting surface under rotation.

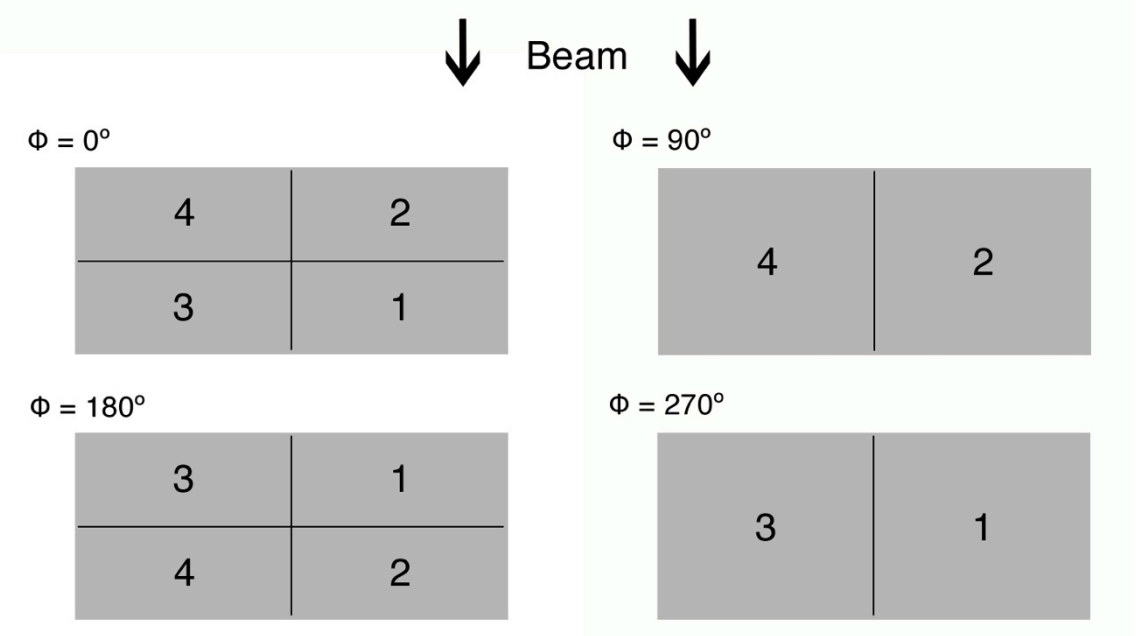

Figure 2.8: Diagram of phi rotation (collectors labeled 1-4)

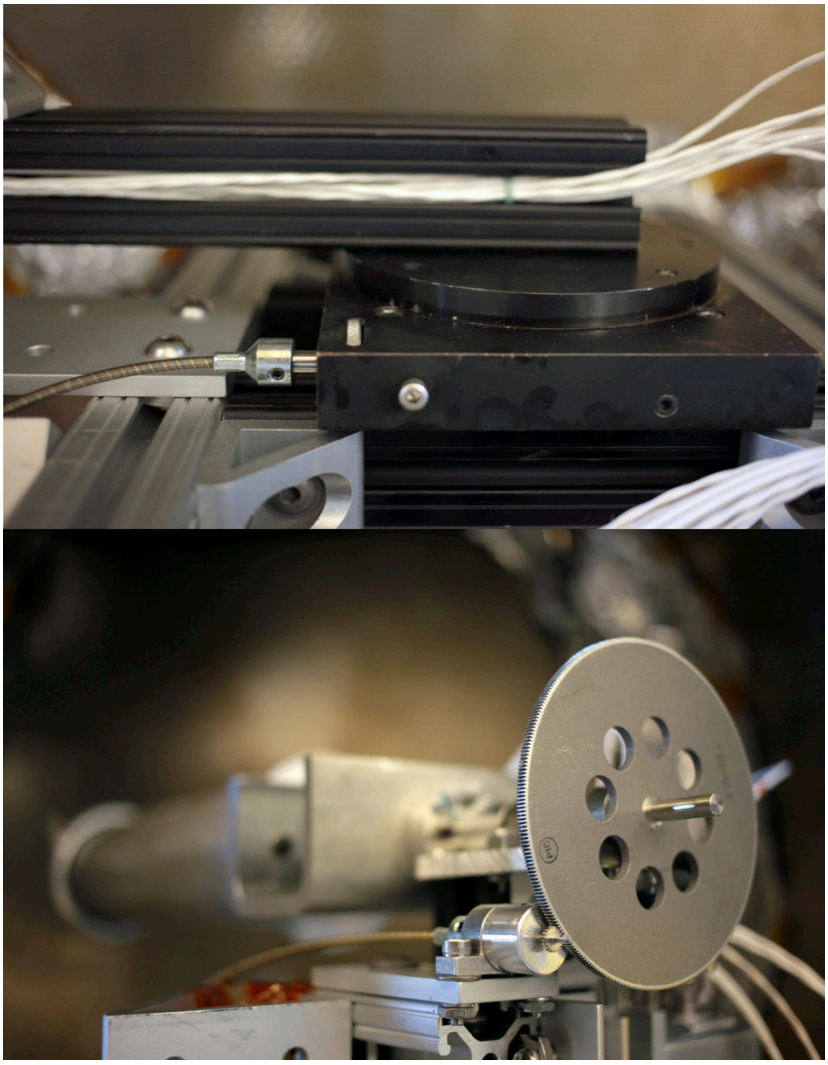

Figure 2.9: Theta (top) and phi (bottom) rotational stages

2.2.2 ILP Electronics Setup

Power supplies were required for multiple components in the experiment. Each of the grids on the ILP required its own power supply. The outer grid was biased using a 0-120 V Hewlett Packard E3612A, the inner grid was biased

using a Bertan Associates Series 230 High Voltage Supply, as the inner grid required higher voltage than the outer grid. The middle grid was swept using a Keithley Model 248 High Voltage Supply, controlled via GPIB. The op-amps inside of the preamp were biased using a ±20 V Hewlett Packard E3630A Triple Output power supply. Other instruments include a Hewlett Packard 34970 Data Acquisition/Switch unit to switch between the four collector signals, and an Agilent 3441A Digital Multimeter to read voltage values from the collector.

This switcher, multimeter, and high voltage supply for the middle grid were all controlled via GPIB by a sweeping program written in Python in part by Magnus Karlsson, Jesse Caldwell, and myself. This code told the middle grid to switch voltage values, then took data on each collector from the multimeter as the switcher cycled through each of the collectors.

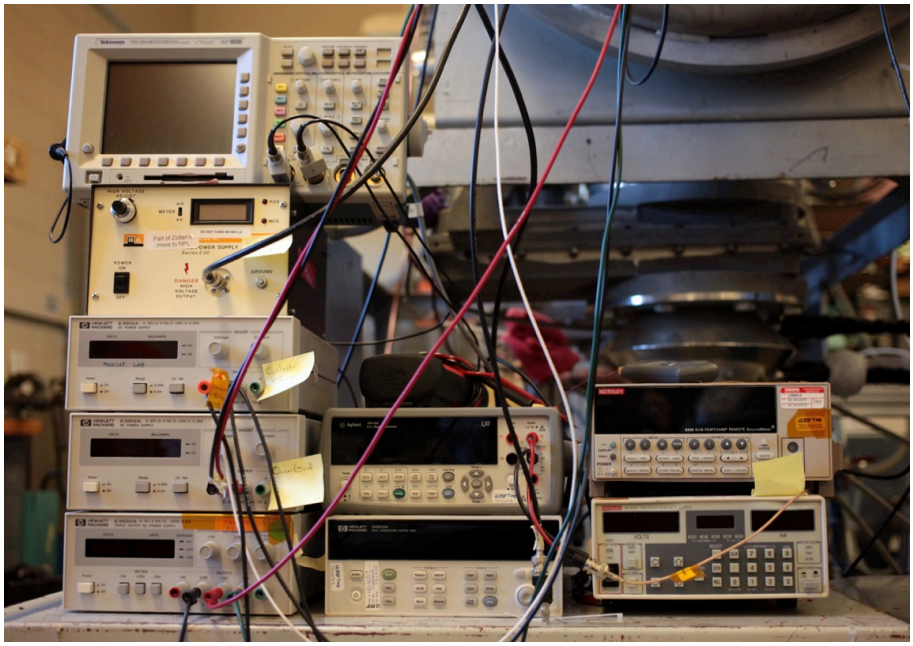

Figure 2.10: Electronic instruments setup
Includes three power supplies for grid biases, power supply for preamp, digital switcher, digital multimeter, and sub-fempto ammeter

All of the signals and power were run through a custom zero-length adapter fabricated by DV Manufacturing. The feedthrough was a 10" CF flange with a 25 pin d-sub, and three 2.75" CF flange mounts.

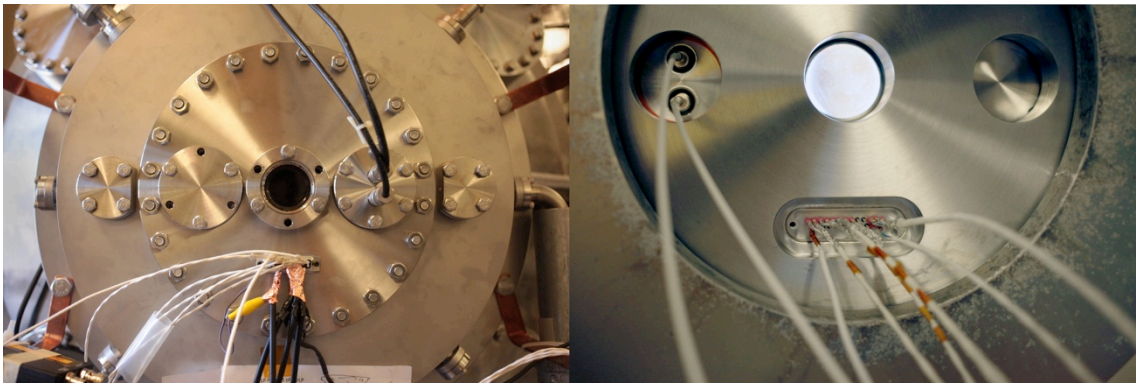

Figure 2.11: Custom electrical feedthrough flange

2.3 Initial Tests – Perfecting the Setup

Once the test stand was setup, initial tests followed. Dr. Xu Wang provided a secondary instrument, the IEA, which allowed us to look at the plasma environment before the prototype ILP was complete. From this we learned that the setup was generally working as expected, however beam current was very high, even at the lower current limit of the ion source. After this, we observed charge exchange and ionized neutrals in the initial tests with the ILP. Experimenting with different gases for the ion source, combined with lowering the pressure in the chamber helped us to achieve the necessary plasma parameters.

2.3.1 Ion Energy Analyzer

The IEA was used both in the early stages of the experiment to characterize the plasma environment before the ILP was ready, and in the later stages of the experiment to look into the issue of beam non-uniformity. The IEA is a planar Faraday cup with a collector surface of 1 cm^2 and three grids in front of the collector. The IEA functions largely the same as the ILP with two electron rejection grids and one ion selection grid. The main difference besides the geometry is that the collecting surface on the IEA is biased, resulting in further rejection of electrons.

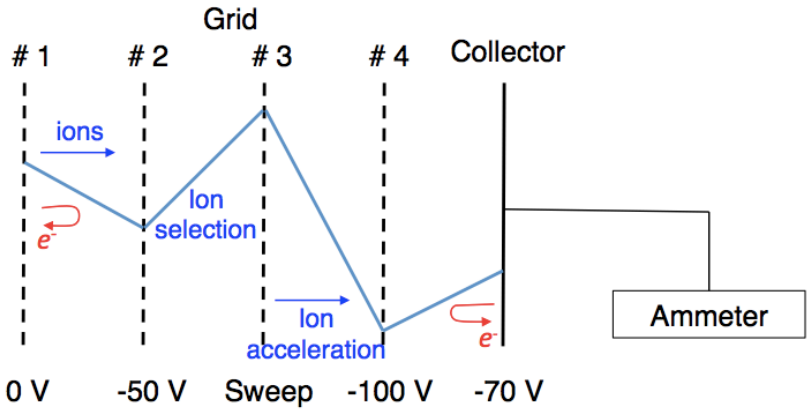

Figure 2.12: Diagram of IEA

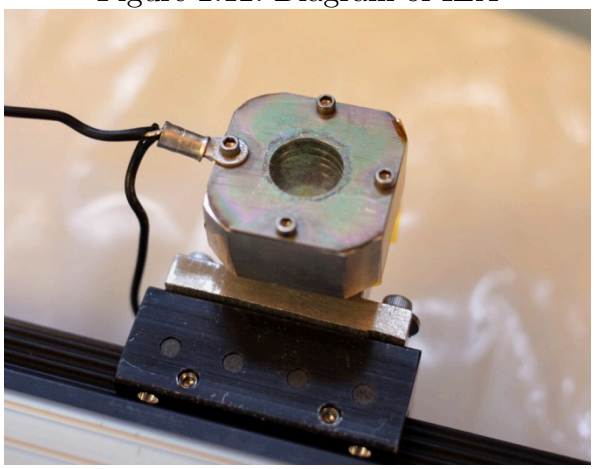

Figure 2.13: Image of IEA

The grids were biased using the same power supplies as the ILP. The collecting surface was biased with a Keithley 6430 Sub-Femptoamp Remote SourceMeter. Code was written in Python to control the SourceMeter and the swept grid voltage by Jesse Caldwell and myself.

Figure 2.14 shows an I-V curve of an ionized He plasma environment, where the x-axis shows the voltage being swept on the middle grid of the IEA. This plot shows functionality of the ion source (ion current at lower voltages and zero current after the grid was swept past 400 V, as the beam energy is 400 eV) and thus, tests with the ILP could begin. Later in the experiment the IEA was placed on a worm drive along the horizontal axis of the ILP and was used to plot non-uniformity in the plasma beam as multiple sweeps were taken across the chamber (results discussed in Chapter 3).

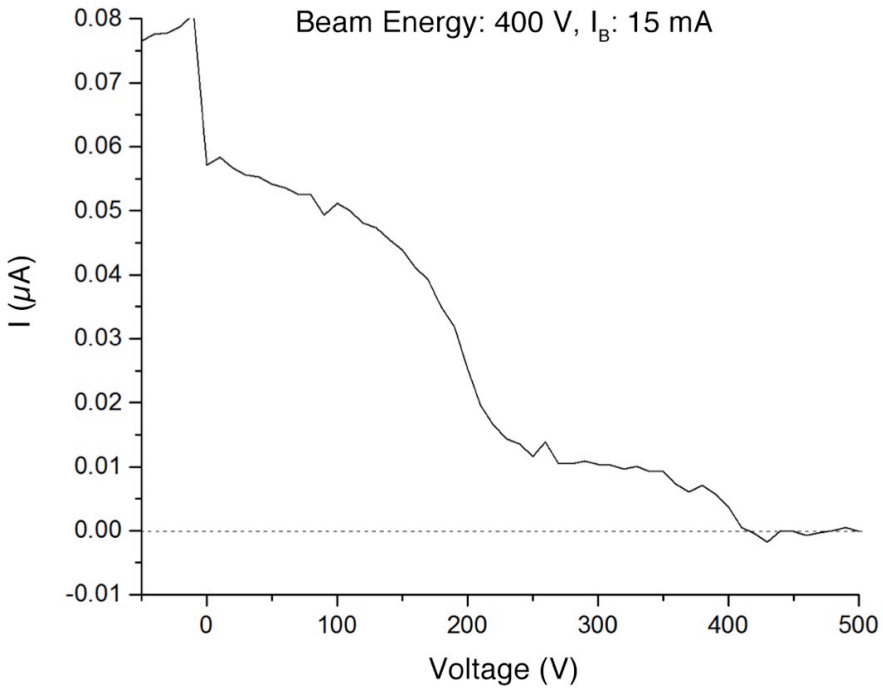

Figure 2.14: IEA I-V curve
Grid 1: 0 V, Grid 2: -50 V, Grid 3: 0-500 V, Grid 4: -100 V, Collector: -70 V

2.3.2 Decreasing Current

Initial tests with the IEA showed minimum current levels of 60 nA/cm^2. Because this did not meet our testing requirements, it was necessary to lower the current. To do this, perforated sheets of steel were mounted onto the rails of the rig. Each attenuator was grounded to the chamber to ensure no charging effects.

With one attenuator in the chamber, the current was shown to drop from 60 nA/cm^2 to 20 nA/cm^2. With four attenuators in the chamber current dropped from 20 nA/cm^2 to 0.5 nA/cm^2. Plots of these sweeps are shown in Figure 2.15. A four-attenuator arrangement was chosen, as it shows current in the noise range for the IEA where the ILP is expected to see signal with its finer resolution. Later in the experiment current was decreased further by adding attenuators in a 10" nipple close to the source after installing the turbo. This had the dual effect of creating a differential pressure in the chamber to lessen negative effects of higher pressure (as discussed in the next sections) and further lowering current.

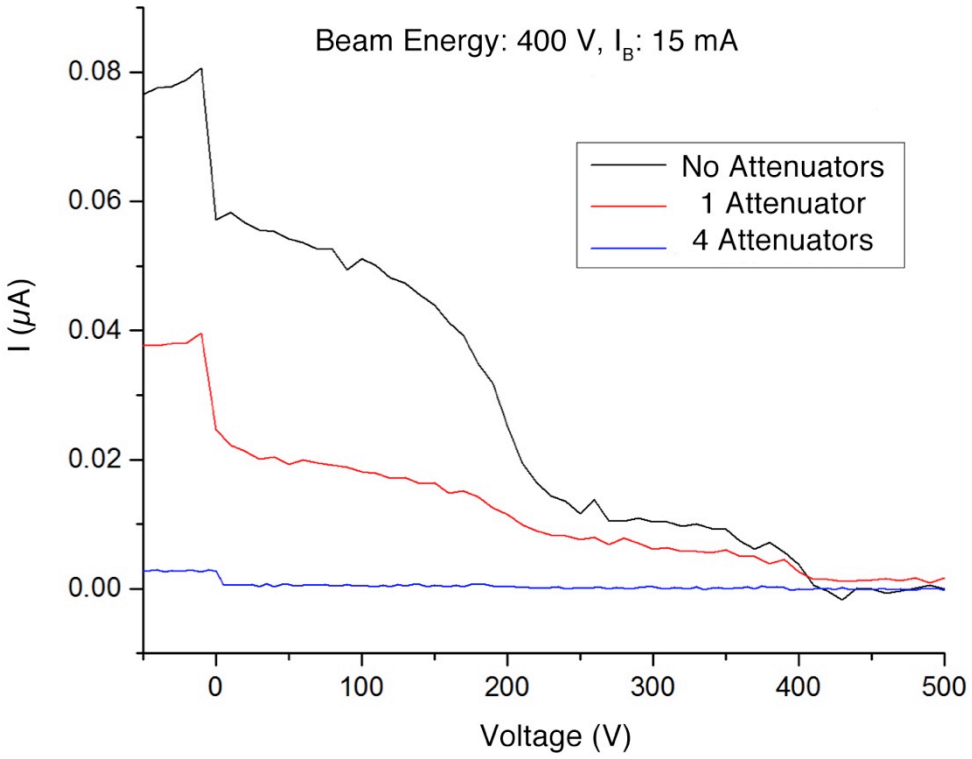

Figure 2.15: I-V Plots of zero attenuators vs. one attenuator vs. four attenuators in chamber with IEA
Grid 1: 0 V, Grid 2: -50 V, Grid 3: 0-500 V, Grid 4: -100 V, Collector: -70 V

Figure 2.16: Perforated steel attenuators

2.3.3 ILP Initial Tests

To tune the experimental setup to fit our particular testing requirements, a series of tests were performed. The main problem that needed to be addressed was the high chamber pressure. With higher pressure there are more neutrals in the chamber causing charge exchange. This can be seen as a spike at lower voltages on I-V curves, and was seen in both the IEA data and the ILP data. Another effect of high pressure is energetic neutrals left over from charge exchange interactions (original charge donors), make their way to a collecting surface and donate an electron via ionization to the collector upon impact. This can be seen as an increased number of electrons past the energy cutoff on an I-V curve (shown in Figure 2.17). Lowering the pressure in the chamber will decrease both of these effects, moving the I-V curves closer to the real ion current from the beam.

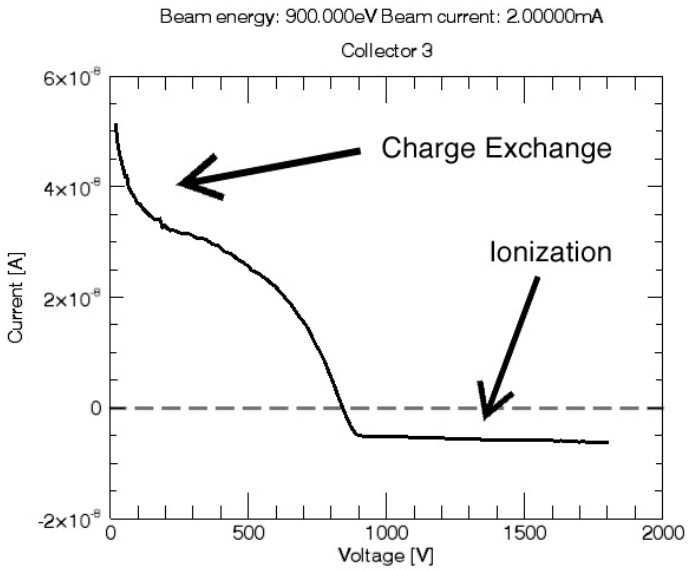

Figure 2.17: Example plot displaying charge exchange and ionization of neutrals. Gas flow rate: 1.1 sccm, Chamber pressure: 3.8×10^{-5} Torr
Outer Grid: -50 V, Middle Grid: 0-1800 V, Inner grid: -200 V

When operating the ion source with helium it was necessary to run at flow rates as high as 6.0 sccm in order to maintain discharge. This corresponded to pressures on the order of 10^{-3} Torr in the chamber. This effect occurred because of helium's smaller cross section and higher ionization energy. As a result of the increased number of neutrals in the chamber, a substantial amount of electron current was seen due to ionization. When we switched to argon we found that the flow rates could be lowered dramatically while still maintaining discharge, as argon has a lower ionization energy and a much larger cross section. Minimum flow rate required to maintain discharge was found to be 0.9 sccm at a pressure of 10^{-5} Torr. A plots comparing He to Ar is shown in Figure 2.18.

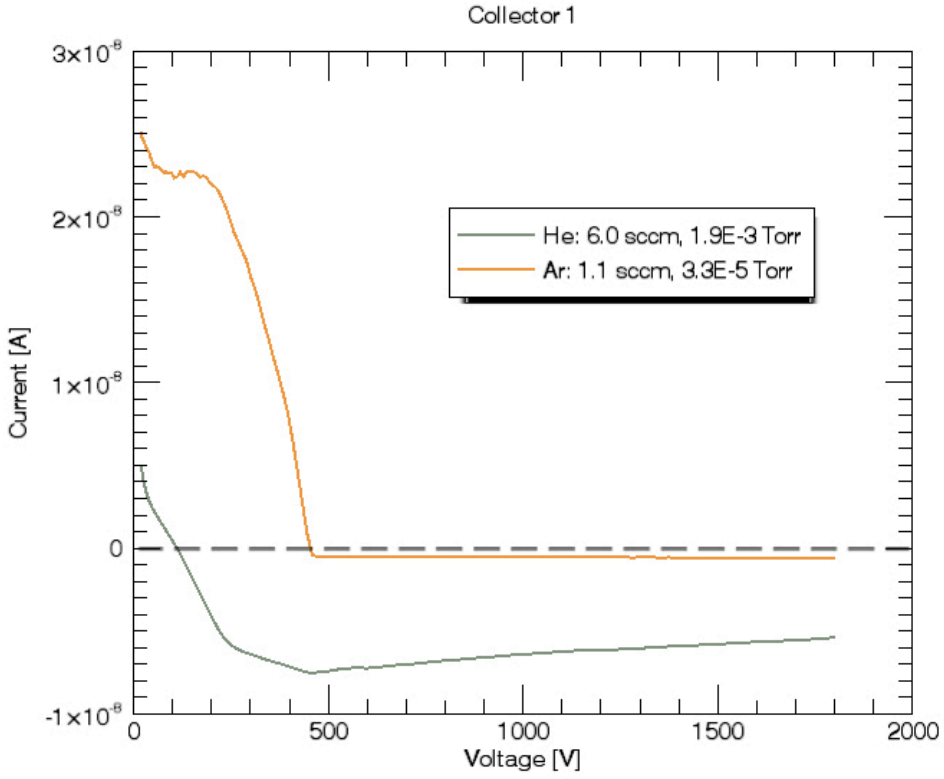

Figure 2.18: Flowing He vs. Ar.
Beam energy: 400 eV, I_{beam_He}: 15 mA, I_{beam_Ar}: 1 mA
Outer Grid: -50 V, Middle Grid: 0-1800 V, Inner grid: -200 V

As is apparent in Figure 2.18, there was still a significant amount of charge exchange occurring at low voltages on the middle grid and a small amount of electron current from ionized neutrals at higher voltages. It was hypothesized that if the pressure was lowered near the ion source, meaning more of the neutrals don't make their way into the chamber, then these effects would be significantly reduced. To accomplish this, the ion source was taken off of the chamber and a cross piece which allowed three more attachments was installed in its place. The crosspiece would have to hold a substantial amount of weight about three feet from where it was attached to the chamber, so a support system was constructed (pictured in Figure 2.19).

Figure 2.19: Turbo support structure

With the support structure assembled and in place, the ion source was mounted to the end of the cross piece while the turbo along with an ion gauge

to measure pressure were mounted to either side. Three attenuating screens were placed in front of the ion source in the cross piece in an attempt to trap neutrals that could otherwise flow into the chamber and get ionized. Knowing the pressure inside of the crosspiece would let us know if the desired differential in pressure between the chamber and the crosspiece had been accomplished. The pressure in the chamber with no gas flowing to the ion source was measured to be twice as large as the pressure in the crosspiece. This tells us that a differential pressure was occurring. Adding the turbo not only lowered the pressure in the cross piece, but lowered our base pressure in the chamber while not running the ion source by 50% or more depending on how long the chamber had been pumping down. These efforts resulted in the desired effect of decreased charge exchange and ionized neutrals, as seen in Figure 2.20.

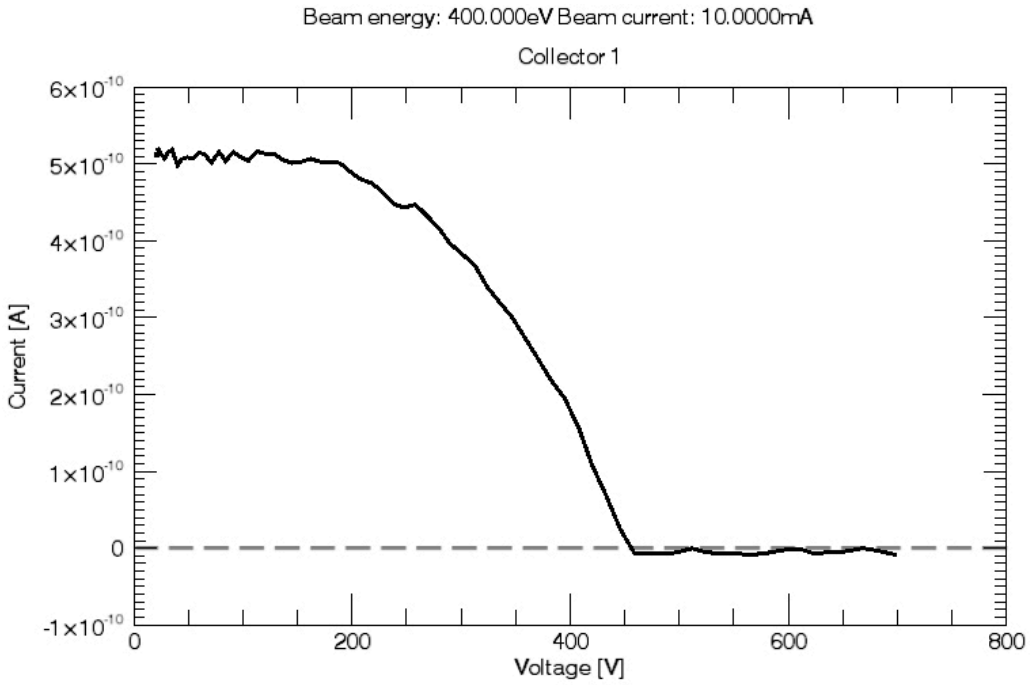

Figure 2.20: Plot with charge exchange and ionized neutrals minimized.
Flow: 0.9 sccm, Pressure: 1.0×10^{-5} Torr, ϑ = -90°, ϕ = 180°
Outer Grid: -50 V, Middle Grid: 0-1800 V, Inner grid: -200 V

With the effects of charge exchange and ionized neutrals minimized, data from the I-V sweeps was then matched to analytical models and a simulation for the CELP NASA proposal (reference 1). Results shown in Figure 2.21 indicate a near perfect matching of experimental data with these models. With the functionality of the experimental setup established, current resolution and angular resolution testing could begin.

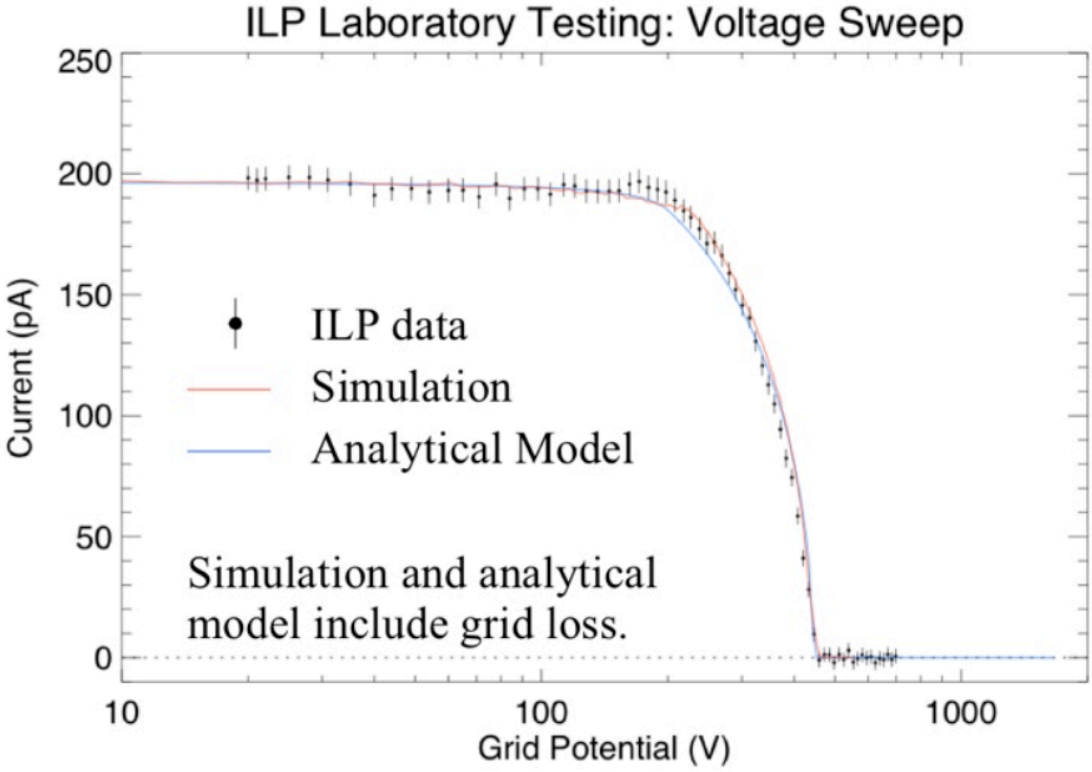

Figure 2.21 [1]: Plot of experimental data with an analytical model and simulation. Beam Energy: 400 eV, Beam Current: 10 mA, Flow 0.9 sccm, Pressure: 1.0×10^{-5} Torr, ϑ = -90°, ϕ = 180° Outer Grid: -50 V, Middle Grid: 0-1800 V, Inner grid: -200 V

Chapter 3

Results

In this chapter a summary of experimental results is presented. Ultra-low current test were preformed to observe low end current capabilities of the ILP. In addition, eight rotational tests were preformed: four for theta and four for phi. Rotations in theta ranged from -90° to 90° with a resolution of ±10°. Rotations in phi ranged from 0° to 360° with a resolution of ±5°. For each rotation, current in the ranges of 100 pA and 10 nA with beam energies of 400 eV and 900 eV was measured.

3.1 Current Resolution

With current resolution goal of 10 pA/cm^2, we take the surface area of one collector and divide the current seen in Figure 3.1 by this value to get our minimum current resolution. We find a minimum current resolution of 0.1 pA/cm^2 (low voltage plateau shown in Figure 3.1 divided by collector surface area),

significantly lower than the expected minimum currents at Europa. This was accomplished using four attenuators in the chamber with three attenuators in the cross piece in front of the ion source.

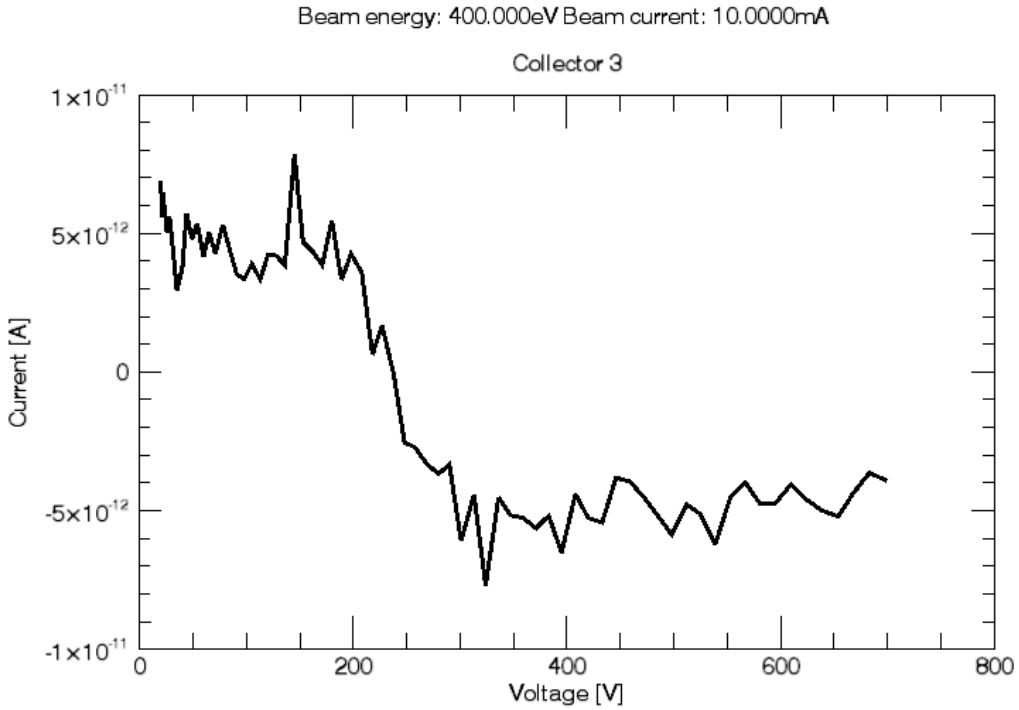

Figure 3.1: I-V plot of minimum current
Beam energy: 400 eV, Beam current: 10 mA, Gas flow rate: 0.9, Chamber pressure: 1×10^{-5} Torr,
ϑ = -90°, ϕ = 332°
Outer Grid: -50 V, Middle Grid: 0-1800 V, Inner grid: -200 V

3.2 Angular Resolution

With 4° steps in theta and 5° steps in phi, our instrument showed a resolution in theta of ±10° and of ±5° in phi [1]. Prof. Robert Ergun computed these results for the CELP NASA proposal. A plot of physical angle vs. derived angle

can be see in Figure 3.2; a clear correlation is seen verifying the instruments functionality in deriving phi.

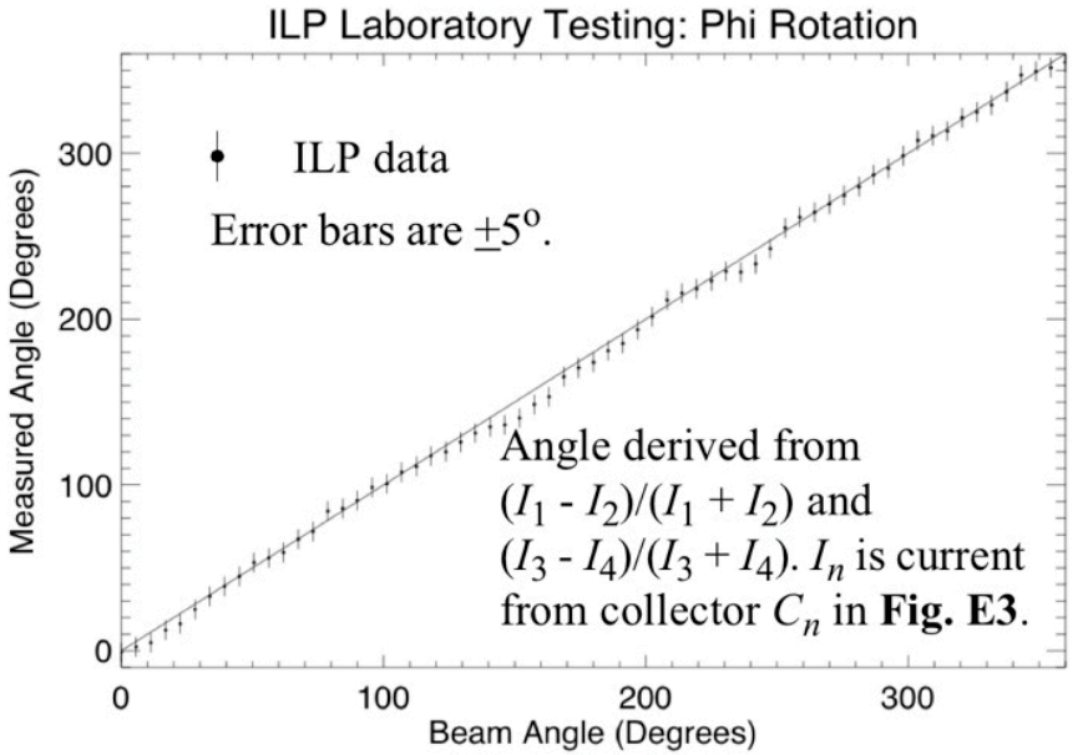

Figure 3.2 [1]: Physical angle vs. derived angle in phi

The primary source of error in the experimental data comes from beam non-uniformity [1]. Seen in Figure 3.3, two side-by-side collectors facing the beam see current values that differ by about a factor of two. This shows that the ion beam is spatially non-uniform. To quantify the non-uniformity more clearly, the IEA was placed on a worm drive and moved horizontally across the chamber. Voltage sweeps were performed in 1 cm steps across the horizontal space occupied by the ILP. Curves were fit with a flat line at low voltages and current values found by the fit were plotted against each other. Using this data, corrections can be made to normalize current.

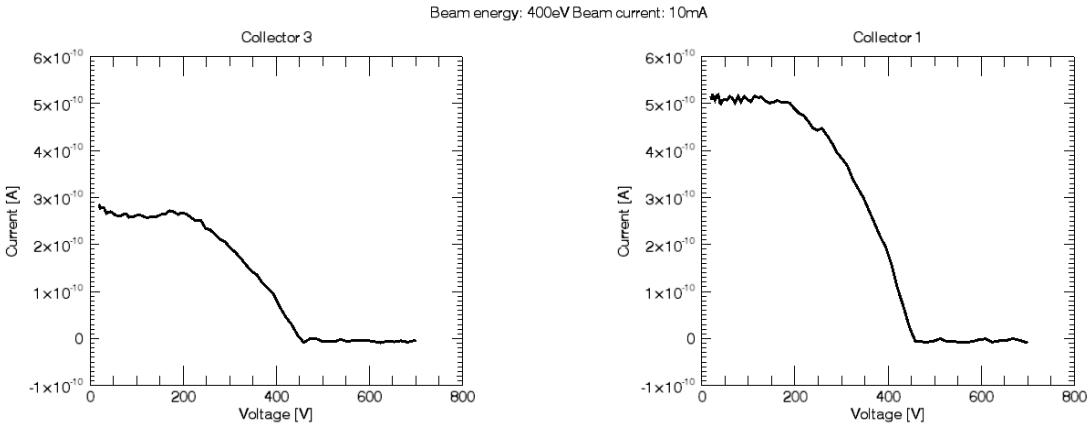

Figure 3.3: Example of unequal currents on front-facing collectors
Flow: 0.9 sccm, Pressure: 1.0×10^{-5} Torr, ϑ = -90°, ϕ = 180°
Outer Grid: -50 V, Middle Grid: 0-1800 V, Inner grid: -200 V

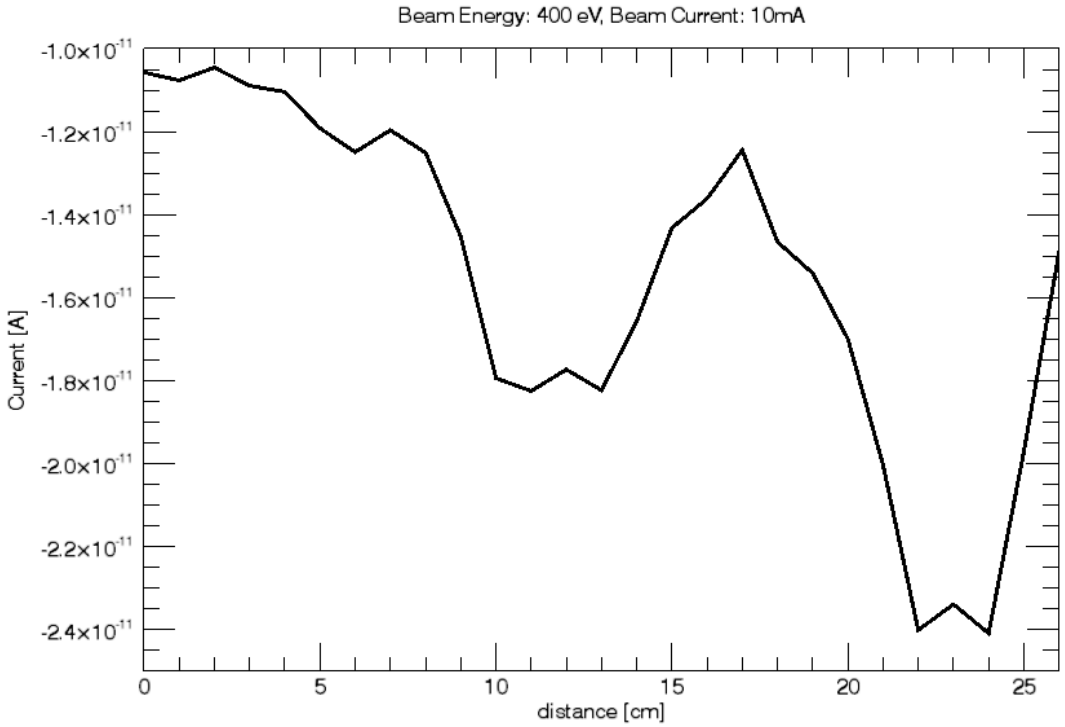

Figure 3.4: IEA beam map

3.3 Conclusions

With our experimental setup, sufficiently low currents were measured by the ILP. The required minimum current of 10 pA/cm^2 was achieved, showing a minimum current resolution of 0.1 pA/cm^2.

Angular resolutions of $\pm 10^\circ$ in theta and $\pm 5^\circ$ in phi were seen in secondary data analysis with error largely due to beam non-uniformity. Experimental results were verified by matching experimental data to a simulation and an analytical model, both with a high degree of success.

Bibliography

[1] F. Bagenal, Colorado Europa Langmuir Probe, 2014, (proposal), Submitted to NASA.

[2] F. Bagenal, R. Ergun, L. Andersson, F. Crary, A Probe for Europa's Plasma Interaction CELP: Colorado Europa Langmuir Probe, 2014, (ICEE), Instrument Concepts for Europa Exploration, Submitted to NASA.

[3] NASA, Europa Clipper, http://solarsystem.nasa.gov/missions/profile.cfm?MCode=EuropaClipper, n.d., (website), Accessed Oct. 2014.

[4] C. Zimmer, Subsurface Oceans on Europa and Callisto: Constraints from Galileo Magnetometer Observations, Icarus **147**, 329 (2000).

[5] K. Khurana and M. Kivelson, Electromagnetic Induction from Europa's Ocean and the Deep Interior, in Europa. Pappalardo, Robert et al. eds. University of Arizona Press, (2009).

[6] J. Saur, D. Strobel, and F. Neubauer, Interaction of the Jovian Magnetosphere with Europa: Constraints on the Neutral Atmosphere, Journal of Geophysical Research (1998).

[7] M. Kivelson, K. Khurana, and M. Volwerk, Europa's Interaction with the Jovian Magnetosphere, in Europa. Pappalardo, Robert et al. eds. University of Arizona Press, (2009).

[8] Pfeiffer Vacuum, TMH 520/TMU 520 Operating Intstructions, n.d., (manual).

[9] Kaufman & Robinson, KDC 100 ION SOURCE MANUAL With Molybdenum Two-Grid Dished Divergent 12-cm Diameter Ion Optics, 2012, (manual).

[10] Kaufman & Robinson Staff, Ion Beam Neutralization, 2006, (Technical Note).